A two-degree-of-freedom hip exoskeleton device for an immature animal model of exercise-induced Legg –Calvé–Perthes disease

J-F Zhang, C-J Yang, T Wu, J-H Li, Z-S Xu and Y Chen

Proceedings of the Institution of Mechanical Engineers, Part H: Journal of Engineering in Medicine 2009 223: 1059
DOI: 10.1243/09544119JEIM597

A two-degree-of-freedom hip exoskeleton device for an immature animal model of exercise-induced Legg–Calvé–Perthes disease

J-F Zhang[1]*, **C-J Yang**[1], **T Wu**[2,3], **J-H Li**[2,3], **Z-S Xu**[2,3], and **Y Chen**[1]

[1]State Key Laboratory of Fluid Power Transmission and Control, Zhejiang University, Hangzhou, People's Republic of China

[2]Sir Run Run Shaw Hospital, affiliated with The School of Medicine, Zhejiang University, Hangzhou, People's Republic of China

[3]Sir Run Run Shaw Institute of Clinical Medicine of Zhejiang University, Hangzhou, People's Republic of China

The manuscript was received on 19 February 2009 and was accepted after revision for publication on 29 June 2009.

DOI: 10.1243/09544119JEIM597

Abstract: Legg–Calvé–Perthes disease (LCPD) is a significant problem in healthcare because it so commonly affects young adults and immature athletes, primarily gymnasts. In this paper, a two-degree-of-freedom (2-DOF) hip exoskeleton device was developed for study on an immature animal model of exercise-induced LCPD. The exoskeleton device can reproduce the repetitive actions and forceful centrality impingements on the coxafemoral head that occur in sports such as gymnastics and acrobatics. It initiated a new method rather than the traditional medical or physiological operation method to establish an animal model of LCPD and allowed for the development and testing of new treatments. Ten immature New Zealand white rabbits were selected for the experiment. Their right legs were driven to achieve repetitive extension/flexion and abduction/adduction beyond the normal range of motion, with centrality impingements at the maximum flexion position, while their left legs were kept in the initial healthy status and acted as the comparing reference. Four weeks later, the basic symptoms of early LCPD of the femoral head appeared. The results of X-ray, magnetic resonance imaging (MRI), gross anatomy observation, and H-E section also revealed it.

Keywords: Legg–Calvé–Perthes disease, exoskeleton, immature New Zealand white rabbits, exercise-induced animal model

1 INTRODUCTION

Legg–Calvé–Perthes disease (LCPD), which bears the name of three different people, Legg, Calvé, and Perthes, who independently described it in 1910, is avascular necrosis (AVN) of the femoral epiphysis and affects young children between the ages of 2 and 12. It is believed that an altered blood supply to the femoral head causes a temporary ischaemia, which leads to an osteonecrosis that may ultimately lead to collapse of the femoral head and altered shape of the hip joint. Although the aetiology is unclear because of the lack of a suitable experimental model [**1**, **2**], researchers have identified certain risk factors. Besides their sex, children with attention deficit hyperactivity disorder, etc., are in general more active than average (running, jumping, sports, etc.) and it has been proved that they may have more possibility for developing LCPD. In fact, repetitive training in gymnastics and errors in technical action have a significant effect on the AVN of the femoral head, which leads many immature gymnastic athletes to suffer from LCPD [**3**, **4**]. Unfortunately, previous attempts to develope an animal model for LCPD or AVN have been based predominantly on determining the vascular aetiology of the disease by means of medical or physiological operation meth-

*Corresponding author: State Key Laboratory of Fluid Power Transmission and Control, Zhejiang University, Hangzhou, 310027, People's Republic of China.
email: caffeezhang@gmail.com

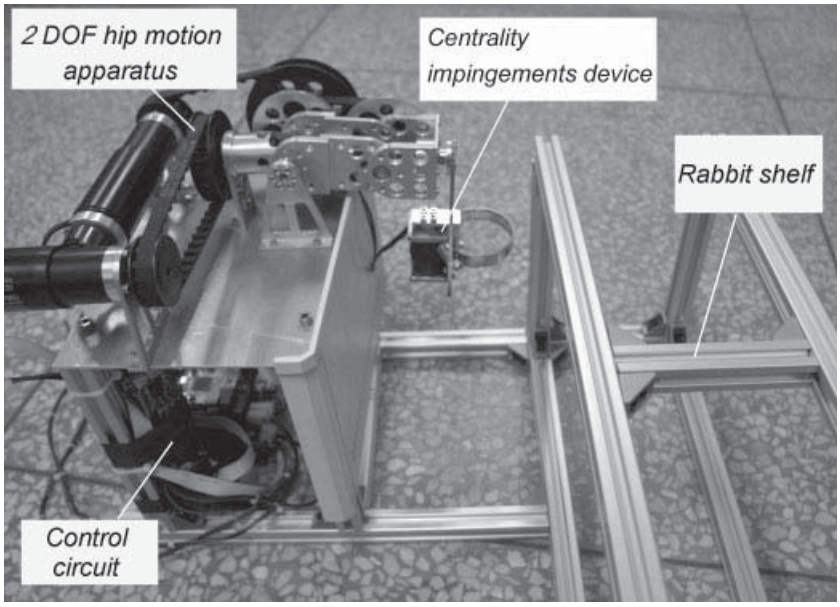

Fig. 1 Overview of the system

ods, in which dislocating the hip joint and ligating the medial and lateral circumflex femoral arteries and veins [**5**], disrupting the blood circulation of femoral heads [**6**], ethanol injection [**7**], and freezing by liquid nitrogen [**8**] are some of the popular methods used to establish animal models focused on rats [**9**, **10**], rabbits [**11**], dogs [**12**], goats [**13**], and even emus [**14**]. There is a need for an animal model that mimics the growth pattern of the proximal femur seen in LCPD. Such a model would allow for the development and testing of new treatments. The bottleneck in establishing a satisfying animal model for LCPD is the lack of an apparatus like the exoskeleton type robotic device designed by Nessler [**15**, **16**] for his study on rodent locomotion after a spinal cord injury. In this paper, a two-degree-of-freedom (2-DOF) exoskeleton apparatus is proposed to meet this requirement. It can provide repetitive actions and forceful centrality impingements (axial loading) on the femoral head, such as those that occur in gymnastics [**17**]. It gives an insight to establish the animal model with qualifying effects of therapeutic interventions on the course of LCPD and paves a new way for analysing its aetiology and the pathogenesis in terms of the gymnastics-like forceful centrality impingements and repetitive actions in order to evaluate new therapeutic treatment. In the research, ten New Zealand white rabbit were treated for passive movement and centrality impingement on the right hip for a long term, while their left legs were kept in the initial healthy status to act as the comparing reference. After 4 weeks, the early symptoms of LCPD appeared. Observations by X-ray, magnetic resonance imaging (MRI), gross anatomy observation, and H-E section all confirmed LCPD.

2 DESIGN OF THE EXOSKELETON DEVICE

Progression towards successful prevention and treatment is hampered by the lack of an experimental animal model that can reliably mimic human LCPD. Most of the effort used to develop an apparatus for establishing a reliable animal model was mainly brought about by the incorporation of two design features. The first key feature is to vividly reproduce the gymnastics-like repetitive actions and forceful centrality impingements. This requires the device to drive the animal subject to achieve the extension/flexion and adduction/abduction of the hip joint beyond its normal range of motion, and to present a case of extensor tendon powerful centrality impingement against the femoral head. The second feature is that the device is required to be firm and lightweight, with as low inertia as possible for a better controlled performance. The concept of exoskeleton devices [**18**–**20**] inspires the system design because of the unique limb–kinematics–anatomy-based design principle [**21**], applying to human power augmentation and rehabilitation.

A photograph of the engineering prototype is shown in Fig. 1. The figure provides an overview of the main components of the system, including a 2-DOF hip motion apparatus, a centrality impingements triggering device, the rabbit shelf, and the control circuit.

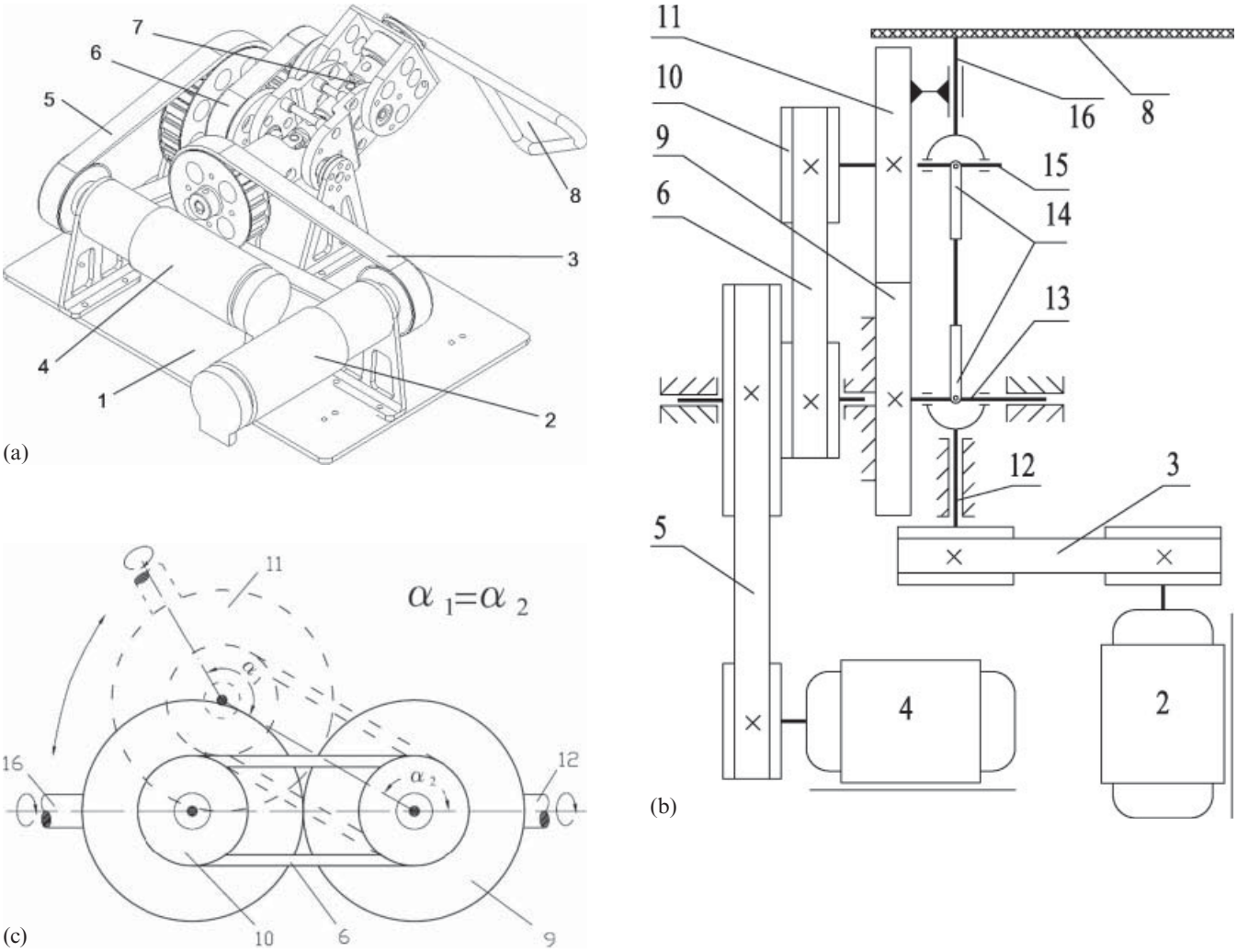

Fig. 2 Prototype of the 2-DOF hip motion apparatus: 1, base; 2, motor for extension/flexion; 3, tooth belt transmission; 4, motor for abduction/adduction; 5 and 6, double tooth belt transmission; 7, flexible shaft; 8, frame; 9, fixed gear; 10, tooth belt wheel; 11, gear; 12, input shaft; 13, axis 1 of the universal joint pair; 14, universal joint pair; 15, axis 2 of the universal joint pair; 16, output shaft

In the 2-DOF motion apparatus, a novel mechanism based on a pair of miniature universal joints is introduced so that two electric motors can both be grounded. Compared with the conventional 2-DOF articulated exoskeleton system where a pair of actuators is employed for each degree of freedom in series, the proposed design decreases the overall inertia of the moving parts in the system. Its basic principle can be explained according to Fig. 2.

1. Motor 2 produces the motion of extension/flexion. Its motion can be transferred to the corresponding motion of frame 8 via the tooth belt 3 and the flexible shaft 7 composed of a pair of universal joints 14.
2. Motor 4 generates the motion of adduction/abduction as its motion can be transferred to the swing of frame 8 around axis 15, which is perpendicular to the axis of extension/flexion.
3. As illustrated in Fig. 2(c), gear 9 is fixed and composes a planetary gear mechanism with gear 11. When the rotation of motor 4 is transmitted to the rotation of belt wheel 10 via two tooth belt transmissions 5 and 6, gear 11 may rotate around the fixed gear 9.
4. Since the radius of both gears is the same and axis 13 and axis 15 of the universal joint pair 14 is concentric to the axis of gear 9 and gear 11 respectively, it makes the input shaft 12 and output shaft 16 of the universal joint pair 14 parallel, namely $\alpha_1 = \alpha_2$, so that the motion on shaft 12 can be transmitted to the frame 8 with high fidelity.

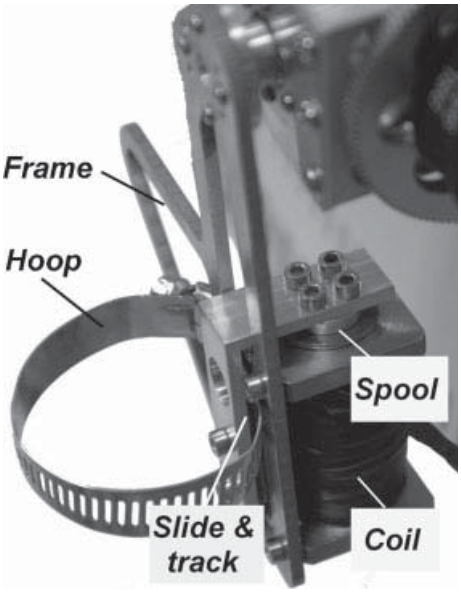

Fig. 3 Device for centrality impingements

The research of Sink *et al.* [**22**] indicates that because gymnasts usually subject their hips to a significant load (up to 10–15 times the weight of the athlete himself/herself), especially when landing a jump, the centrality impingement against the femoral head becomes a key point for inducting LCPD as well. In order to establish a similar animal model, the proposed device should be able to generate centrality impingements that are up to 10 times the weight of the rabbit. This presents an engineering challenge. Here a solenoid-based device, widely utilized to generate a large force instantly [**23**], is adapted. The main idea in power elevation is to store energy in a large capacitor and then discharge it instantly when the solenoid is activated. By passing a large current, the solenoid pushes a steel rod straight forward, emitting a huge impingement. By controlling the time the capacitor's voltage is induced into the solenoid, the magnitude of the impingement can be adjusted. Therefore, a pulse width modulation (PWM) signal is put on a MOSFET to adjust the flow of current through it as well as the intensity of impingements.

Figure 3 outlines the device for centrality impingements. The shank of the rabbit leg is fastened on the frame with neoprene straps and the thigh of rabbit is attached to the spool by holding together both ends of a hoop. Therefore, the centrality impingement generated by the solenoid can be forced on to the femoral head of the hip. With the system performance test, it is observed that the centrality impingement produced by the solenoid is up to about 200 N.

3 IMPLEMENTATION OF THE CONTROL SYSTEM

The set-up of the system is illustrated in Fig. 4(a). The 2-DOF device for the motion of extension/flexion and adduction/abduction is driven via a toothed belt by two grounded d.c. motors (Maxon^{TM} RE36, Interelectric AG, Switzerland). Encoders are mounted on both motors to measure the angles. Therefore, an individual position close control loop was implemented for each drive. CAN bus bridges the PC and small-sized full digital smart motor controllers (Maxon^{TM} EPOS 24/5, Interelectric AG, Switzerland). The motion pattern and desired speed can be adjusted. A control board based on ATMEL mega 128 MCU is designed to receive the command from the PC via RS232 and to implement the closed-loop centrality impingement control.

Since this device is used by researchers or physiotherapists, the GUI must be friendly and easy to use. Figure 4(b) shows the GUI programmed by LabVIEW^{TM}, National Instruments, USA. It includes the column of system configuration, a system parameter setting, operating panel, and data real-time display. The operator can easily adjust the settings on the GUI, and the system performance can be displayed on the right screen in real time. Additionally, a database is developed to record the system settings and the experiment data as well.

4 EXPERIMENTS AND DISCUSSIONS

4.1 Performance of the system

In the experiments, the capability of the exoskeleton device is first evaluated. The device was commended to follow a predefined trajectory repetitively. The angular range of the motion for extension/flexion and adduction/abduction were both larger than the normal ranges of the rabbit. The mean performance, as shown in Fig. 5(a), satisfied the requirement for the average error to be less than 0.01 rad (Fig. 5(b)).

Then the exoskeleton device ran in the form of extension/flexion from $-2\pi/3$ to $2\pi/3$ rad at different moving speeds (2π, 4π, 6π, 8π, and 10π rad/s), while impingements were generated with the flexion to $2\pi/3$ rad. The same procedure was repeated a hundred times for all five speeds, resulting in a total of 500 trials. Results of the mean angles and mean impingements were plotted in Fig. 5(c). The present results indicate that the system had solid performances in the first four cases while

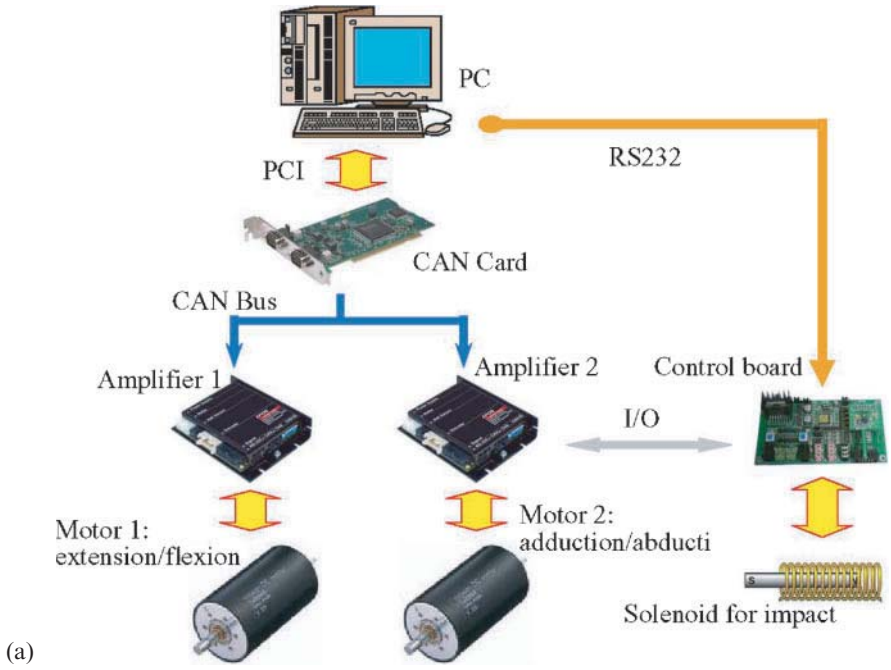

(a)

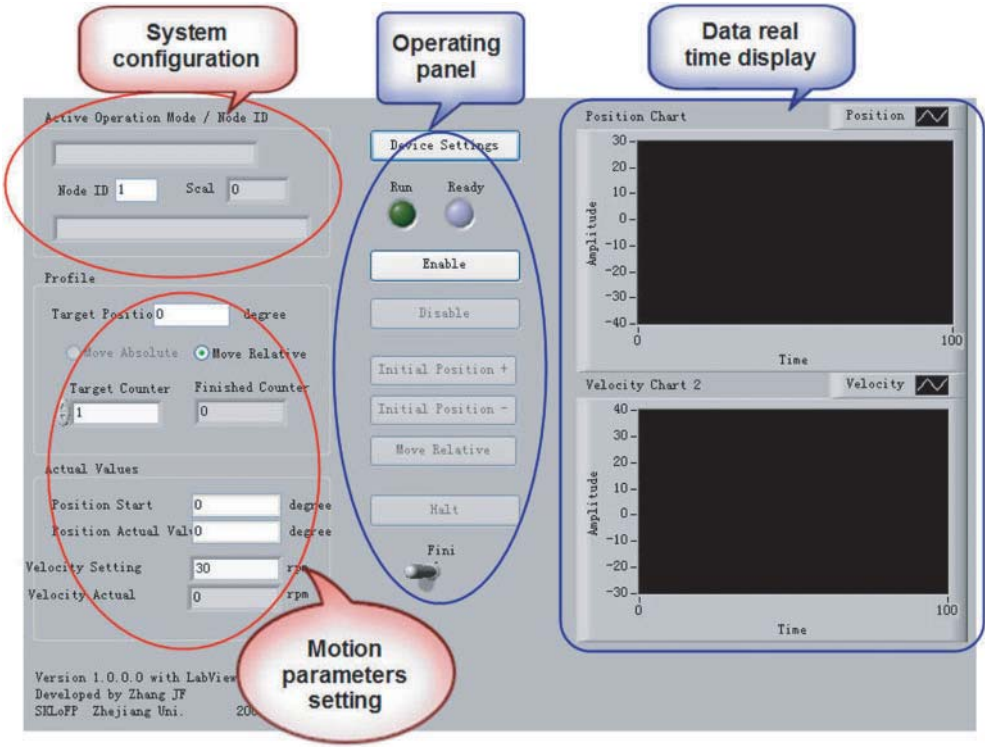

(b)

Fig. 4 Implementation of the control system. (a) Architecture of the control system and (b) guest graphical user interface (GUI)

the magnitude of the centrality impingement decreased to about 160 N when the moving speed was 10π rad/s. As a result, the existing system was advised to be utilized at the speed range of 2π to 8π rad/s.

4.2 Animal model establishing experiments

A total of ten healthy immature New Zealand white rabbits (mean age: 11 weeks; range: 10–12 weeks; weight: 1.51 ± 0.22 kg) were selected. Their epiphyses

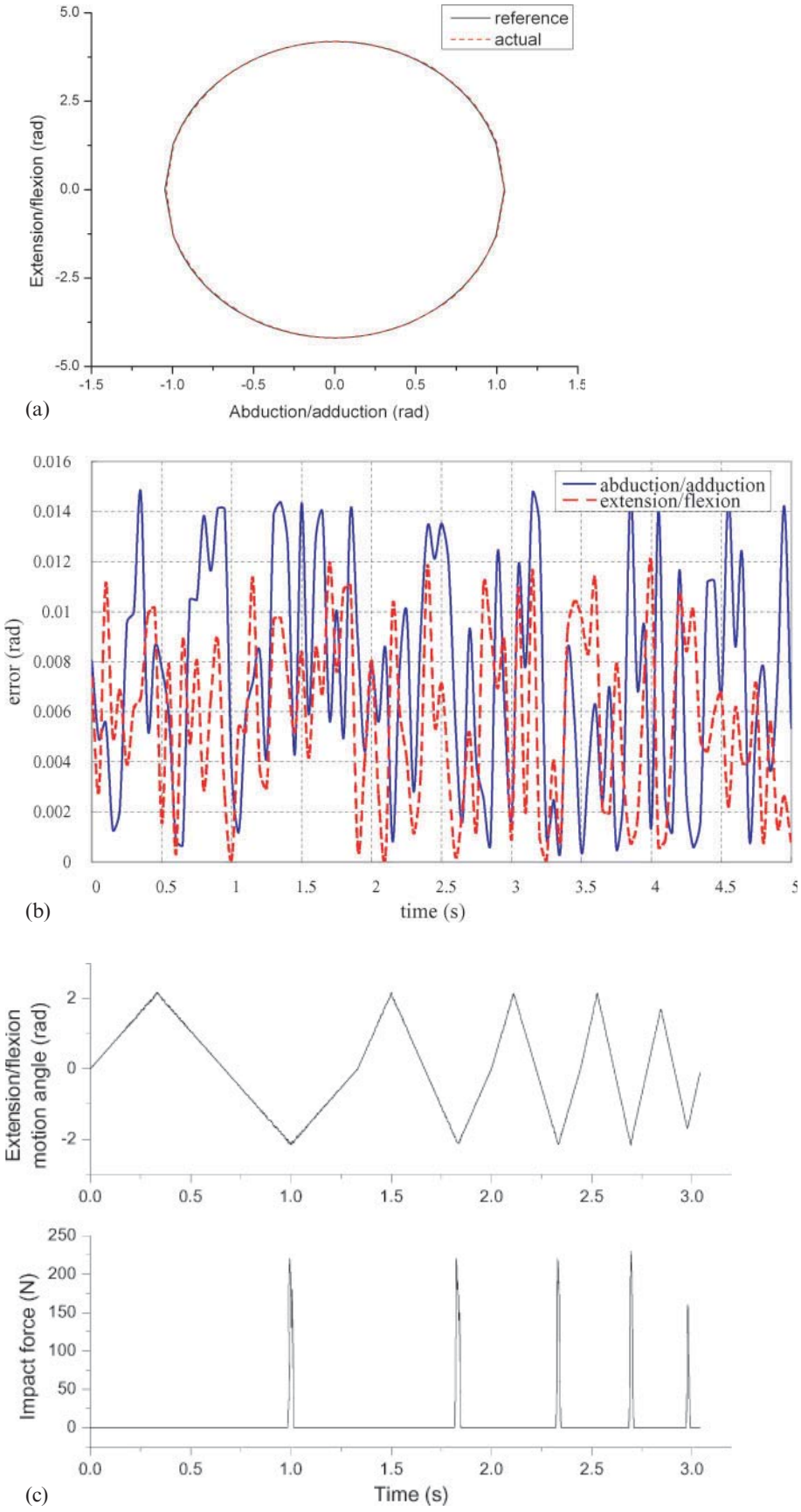

Fig. 5 Characterization of the exoskeleton system within sets of experiments. (a) Result of trajectory tracking, (b) tracking error, and (c) mean angles and mean impingements

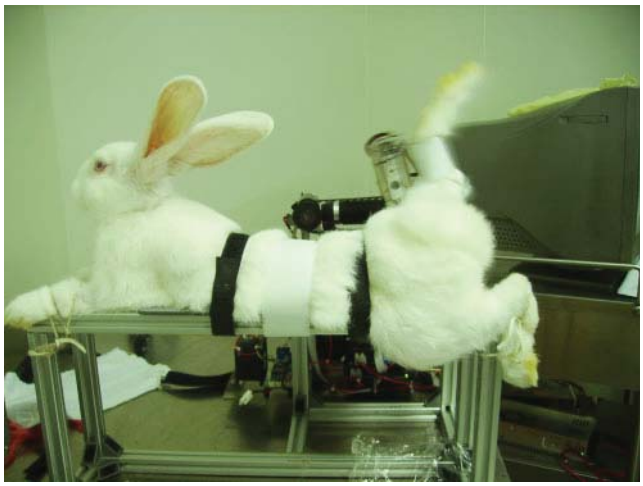

Fig. 6 Animal model inducing experiment

were proved not to be closed by X-ray. They were driven to achieve the extension/flexion and adduction/abduction of the hip joint beyond its normal range of motion accompanied by centrality impingements, with the aim to induce LCPD on their right hips, while the left legs were kept in the initial healthy status, acting as the comparing reference, as shown in Fig. 6. All experimental procedures were approved by the Animal Care Committee of the hospital and all rabbits were monitored closely by the veterinary staff in the hospital during the experimental session. The rabbit right leg was fixed on the frame of the exoskeleton as introduced above, and driven passively in extension/flexion (range: $-2\pi/3$ to $2\pi/3$ rad) and abduction/adduction (range: $-\pi/3$ to $\pi/3$ rad) repetitively at a moving speed of 4π rad/s. Centrality impingements were triggered as often as the rabbit hip was driven to flex to $2\pi/3$ rad. For every animal subject, the experiment was carried out 4 hours a day with more than 1000 centrality impingements, over a period of 4 weeks.

4.3 Observation

Unfortunately the first two rabbits were sacrificed after 3 days, while the remaining eight experimental subjects, following 4 weeks of experiments, were successfully treated to evaluate the early symptoms of LCPD by X-ray, MRI, gross anatomy observation, and H-E sections. The results were encouraging.

X-ray analysis (Fig. 7(a)) revealed changes in the shape of the operated right femoral head compared with the non-operated left femoral head. A zone of increased bone intensity appeared on the affected side (narrow arrow) associated with the collapse of the femoral head and ambiguous mild osteoporosis

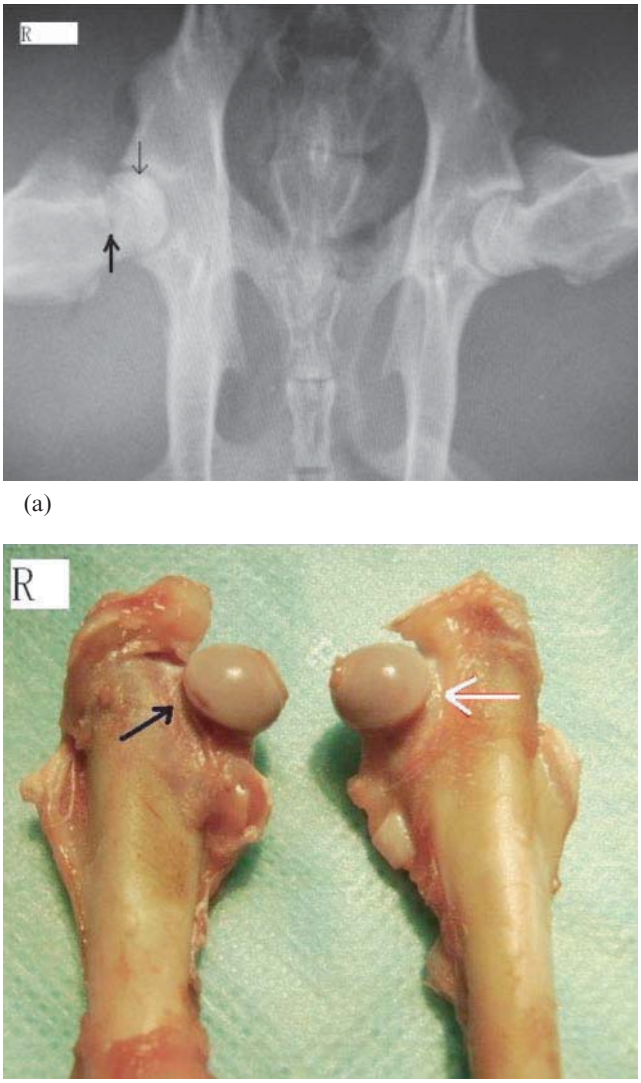

(a)

(b)

Fig. 7 X-ray image and gross anatomy sample of the subject after 4 weeks. (a) X-ray image and (b) gross anatomy sample

(broad arrow) of the trabecular bone, which can clearly be observed in the gross anatomy sample (Fig. 7(b)).

The early diagnosis was also confirmed by MRI scans obtained by a 1.5-T cryogenic imaging system (Magneton Vision, Siemens, Germany). The acquisition matrix was 256×128 and the section thickness was 3 mm. The T1 weighted image (T1WI) (TR, 480 ms; TE, 17 ms) showed decreased signal intensity (arrow in Fig. 8(a)) in the right epiphysis and femoral neck. The T2WI (TR, 3800 ms; TE, 85 ms) revealed that joint effusion diffusely presented in a band-like, a shuttle-like, and an arc zone with increased signal intensity in the joint capsule (narrow arrow in Fig. 8(b)), and formed a sheet of decreased signal intensity with a farraginous increased intensity

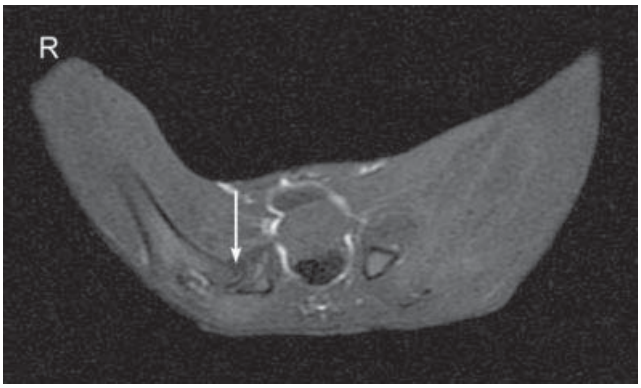

(a)

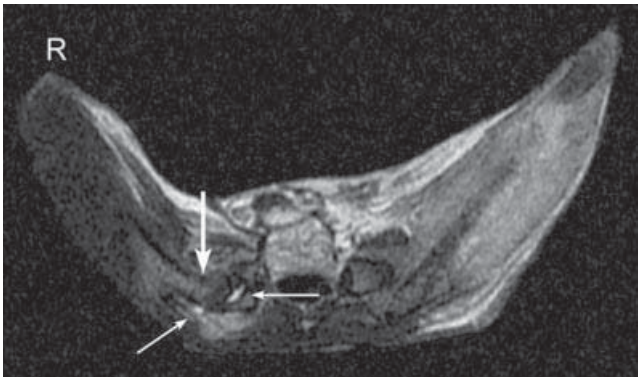

(b)

Fig. 8 MR images of a rabbit hip femoral head. (a) T1WI and (b) T2WI

signal (broad arrow in Fig. 8(b)) as well. These show the incidence of early symptoms in the course of LCPD [**24**, **25**].

In H-E section (see Fig. 9), there was a mount of inflammatory cells mainly composed of lymphocytes. A few adipose cells occurred and replaced the intra-bone marrow in the intra-bone marrow cavity. These phenomena identified with symptoms of early AVN of the femoral head.

5 CONCLUSIONS

The proposed 2-DOF exoskeleton device opens new experimental prospects for studying an immature animal model of exercise-induced LCPD. The key design principles that it incorporates are to drive the animal subject to achieve the repetitive 2-DOF hip actions, in terms of extension/flexion and abduction/adduction associated with centrality impingements on the coxafemoral head, as well as light, low inertia for a better control performance. The real-time control system promises a solid performance with high accuracy and the friendly GUI programmed by LabVIEW also makes it easy to use.

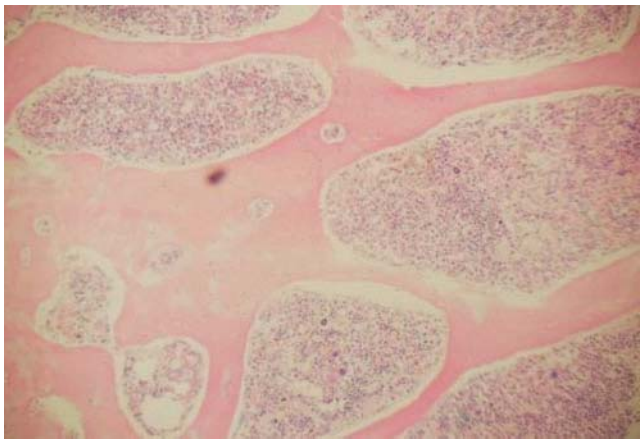

(a)

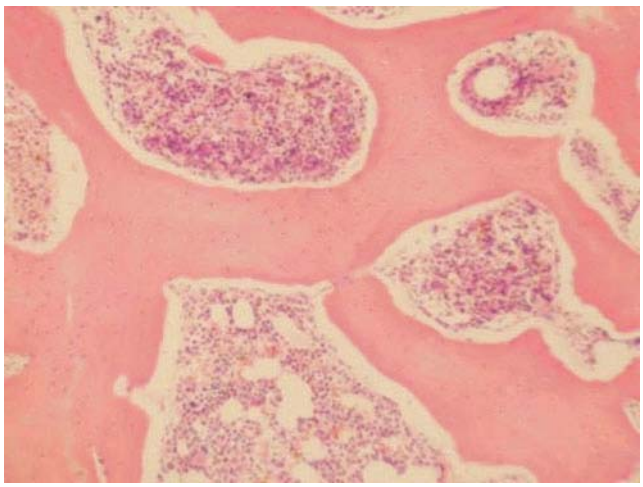

(b)

Fig. 9 H-E section showing a histological specimen of the femoral head after 4 weeks. (a) $\times 40$ and (b) $\times 100$

With the help of this device, the experiments for the study on an animal model of exercise-induced LCPD were carried out. Ten New Zealand White rabbits were primarily tested. The results of the pilot study were encouraging. Despite the sacrifice of two rabbits after 3 days, the symptoms of early LCPD were successfully observed on the remaining eight experimental subjects. The observations of X-ray, MRI, gross anatomy observation, and H-E sections verified this and significantly demonstrated the capabilities of the exoskeleton device.

However, neither severe distortion nor collapse appeared on the rabbits. The reason may be that the rabbit moves in quadrupedal gait instead of bipedal stepping. It will be of interest to study biped stepping in future work, which requires that the animal be placed in a more upright posture to support its weight. This study provides the basis for

further research to develop a successful biped animal model. In addition, it is expected that the exoskeleton device will act as a small-scale test-bed for determining the aetiology and pathogenesis that will optimize therapeutic techniques in the treatment of LCPD in humans.

ACKNOWLEDGEMENTS

The support provided for the research project by the Zhejiang Province Sports Bureau, China ([2006]477) is greatly appreciated. The contributions of the following other members of the project team are gratefully acknowledged: Dong Yi-ming and Zhang Yu.

REFERENCES

1 **Lavernia, C. J., Sierra, R. J.,** and **Grieco, F. R.** Osteonecrosis of the femoral head. *J. Am. Acad. Orthop. Surgeons*, 1999, **7**, 250–261.
2 **Mont, M. A.** and **Hungerford, D.** Non-traumatic avascular necrosis of the femoral head. *J. Bone Jt Surg. Am.*, 1995, **77**, 459–474.
3 **Pallia, C. S., Scott, R. E.,** and **Chao, A. D.** Traumatic hip dislocation in athletes. *Current Sports Medicine Reports*, 2002, **1**, 338–345.
4 **Robert, A. N.** Intra-articular disorder of the hip in athletes. *Physical Therapy in Sports*, 2004, **5**, 17–25.
5 **Nishino, M., Matsumoto, T., Nakamura, T.,** and **Tomita, K.** Pathological and hemodynamic study in a new model of femoral head necrosis following traumatic dislocation. *Arch. Orthop. Trauma Surg.*, 1997, **116**(5), 259–262.
6 **Peskin, B., Shupak, A., Levin, D.,** and **Zinman, C.** *et al.* Chondrolysis in rats with vascular deprivation-induced osteonecrosis of the femoral neck. *Eur. J. Orthop. Surg. Traumatol.*, 2001, **1**(11), 15–20.
7 **Manggold, J., Sergi, C., Becker, K., Lukoschek, M.,** and **Simank, H. G.** A new animal model of femoral head necrosis induced by intraosseous injection of ethanol. *Laboratory Animals*, 2002, **36**, 173–180.
8 **Takaoka, T., Yoshioka, T., Hosoya, T., Ono, K.,** and **Takase, T.** The repair process in experimentally induced avascular necrosis of the femoral head in dogs. *Arch. Orthop. Trauma Surg.*, 1981, **99**, 109–115.
9 **Little, D. G., Peat, R. A., McEvoy, A., Williams, P. R., Smith, E. J.,** and **Baldock, P. A.** Zoledronic acid treatment results in retention of femoral head structure after traumatic osteonecrosis in young wistar rats. *J. Bone Mineral Res.*, 2003, **18**(11), 2016–2022.
10 **Hirano, T., Iwasaki, K.,** and **Yamane, Y.** Osteonecrosis of the femoral head of growing, spontaneously hypertensive rats. *Acta Orthop. Scand.*, 1998, **59**, 530.
11 **Yamamoto, T., Hirano, K., Tsutsui, H., Sugioka, Y.,** and **Sueishi, K.** Corticosteroid enhances the experimental induction of osteonecrosis in rabbits with Shwartman reaction. *Clin. Orthop.*, 1995, **316**, 235–243.
12 **Nishino, M., Matsumoto, T., Nakamura, K.,** and **Tomita, K.** Pathological and hemodynamic study in a new model of femoral head necrosis following traumatic dislocation. *Arch. Orthop. Trauma Surg.*, 1997, **116**, 259–262.
13 **Newton, B., Crawford, C. J., Powers, D. L.,** and **Allen Jr, B. L.** The immature goat as an animal model for Legg–Calvé–Perthes disease. *J. Investigative Surg.*, 1994, **7**(5), 417–430.
14 **Conzemius, M. G., Brown, T. D., Zhang, Y. D.,** and **Robinson, A. R.** A new animal model of femoral head osteonecrosis: one that progresses to human-like mechanical failure. *J. Orthop. Res.*, 2006, **20**(2), 303–309.
15 **Nessler, J. A., Reinkensmeyer, D. J., Timoszyk, W. K.,** and **Nelson, K.** The use of a robotic body weight support mechanism to improve outcome assessment in the spinal cord injured rodent. In Proceedings of the 25th Annual International Conference of the IEEE EMBS, Cancun, Mexico, 17–21 September 2003, pp. 1629–1632.
16 **Nessler, J. A., Timoszyk, W., Merlo, M., Emken, J. L., Minakata, K., Roy, R. R., de Leon, R. D., Edgerton, V. R.,** and **Reinkensmeyer, D. J.** A robotic device for studying rodent locomotion after spinal cord injury. *IEEE Trans. Neural Systems and Rehabilitation Engng*, 2005, **13**(4), 497–452.
17 **Larson, C. M., Swaringen, J.,** and **Morrison, G.** Evaluation and management of hip pain: the emerging role of hip arthroscopy. *The Physician and Sportsmedicine*, 2005, **33**(10), 26–32.
18 **Pons, J. L.** *Wearable robots: biomechatronic exoskeletons*, 2008 (John Wiley & Sons Ltd, Chichester).
19 **Dollar, A. M.** and **Herr, H.** Lower extremity exoskeletons and active orthoses: challenges and state-of-the-art. *IEEE Trans. Robotics*, 2008, **24**(1), 1–15.
20 **Zhang, J. F., Yang, C. J.,** and **Chen, Y.** Exoskeleton arm with force feedback for robot bilateral teleoperation. *Prog. Nature Sci.*, 2007, **17**(9), 56–62.
21 **Yang, C. J., Zhang, J. F., Chen, Y., Dong, Y. M.,** and **Zhang, Y.** A review of exoskeleton type systems and their key technologies. *Proc. IMechE, Part C: J. Mechanical Engineering Science*, 2008, **222**(C8), 1599–1612. DOI: 10.1243/09544062JMES936.
22 **Sink, E. L., Gralla, J., Ryba, A.,** and **Dayton, M.** Clinical presentation of femoroacetabular impingement in adolescents. *J. Pediatric Orthopaedics*, 2008, **28**(8), 806–811.
23 **Jiang, W. L., Wang, W. F., Xiong, R.** *et al.* TDP of ZJUNLICT 2007. In *Proceedings CD of RoboCup 2007*, Atlanta, Georgia, July 2007 (Springer-Verlag).

24 **Sakamoto, M., Shimizu, K., Iida, S., Akita, T., Moriya, H.,** and **Nawata, Y.** Osteonecrosis of the femoral head: a prospective study with MRI. *J. Bone Jt Surg. Br.*, 1997, **76**, 213–219.

25 **Ranner, G., Ebner, F., Fotter, R., Linhart, W.,** and **Justich, E.** Magnetic resonance imaging in children with acute hip pain. *Pediatr. Radiol.*, 1989, **20**, 67–71.